**Proceedings of the ASME 2010 3rd Joint US-European Fluids Engineering Summer Meeting and 8th International Conference on Nanochannels, Microchannels, and Minichannels**
**FEDSM-ICNMM2010**
**August 1-5, 2010, Montreal, Canada**

# FEDSM-ICNMM2010-30736

# SELF-ADAPTIVE UPWINDING FOR LARGE EDDY SIMULATION OF CROSS-FLOW JETS

**Vimal Kumar**
Department of Mechanical & Industrial Engineering, Concordia University,
Montreal, Quebec, CANADA, H3G 1M8

**Marius Paraschivoiu**
Department of Mechanical & Industrial Engineering, Concordia University,
**Montreal, Quebec, CANADA, H3G 1M8**

## ABSTRACT

A self-adaptive upwinding method for large eddy simulation (LES) has been describe in cross-flow in jets. The method is an extension of an existing Reynolds-averaged Navier–Stokes (RANS) code to an LES code by adjusting the contribution of the upwinding term to the convective flux. This adjustment is essentially controlled by reducing the upwind contribution in Roe MUSCL scheme. For the comparison of flow profiles obtained from the self-adaptive upwind LES code the experimental measurements of Andreopoulos and Rodi [1] are considered. The jet-to-cross-flow velocity ratio considered is 0.5 at a Reynolds number of 20,500 based on the jet bulk velocity and the jet diameter. In general, a reasonable agreement with the measurements is obtained. However, an intense backflow near the flat wall is observed. Further a vortex formation is observed behind at a distance of 0.6D from the jet axis.

## INTRODUCTION

The jet in cross-flow (JICF) is a basic flow field which is relevant to a wide variety of applications including fuel injectors, oil refineries, chemical plants, film cooling on turbine blades and etc. In industrial furnaces the jets are used for cross-flow air injection into the incomplete combustion products, i.e. to control the pollutant emissions such as nitrogen oxides ($NO_x$), carbon monoxide (CO), and carbon dioxide ($CO_2$). The cross-flow air jets introduce rapid mixing, and therefore freeze pollutant formation. Therefore it is required to get an accurate knowledge of the fluid flow structures in order to design highly efficient, safe and low-emission combustor.

During the last decade, many experimental as well as numerical studies have shown that the presence of three-dimensional and unsteady vortical structures provides a very efficient mechanism for the fluid flow and mixing process between the jet and the cross-flow. Various numerical schemes (Baldwin-Lomax model, Reynolds-Averaged Navier–Stokes equations) used to report the complex vortical structures in the near field (near the injection rows and the leading edge regions) and in the jet region were found unsatisfactory because these models provide overly simplistic predictions for the complex flow field. A complete direct simulation for the jet in cross-flow is beyond the computing capabilities. Large-Eddy Simulation (LES) is being preferred over other models to capture the flow fields near jet injection and leading edge regions of the JICFs, because of LES's capability in describing unsteady large scale motions and turbulent mixing [2, 3].

In the present paper, the 2$^{nd}$ order Roe-MUSCL flux calculation ($\beta\gamma$ scheme) for large eddy simulations is used to evaluate and possibly control the effects of its numerical dissipative error. In MUSCL ($\beta\gamma$ scheme), the contribution of the upwinding term is adjusted, using a coefficient ($\gamma$) which is directly multiplied into that term during the flux calculation. Coefficient ($\beta$) is also used in order to predict the value of variables at the boundaries of control volume cells.

A complete analysis of the Roe-MUSCL ($\beta\gamma$) scheme's accuracy and its relation to the structure of generated grid has been reported by Carpentier [4]. He concluded that lowering the upwinding coefficient, $\gamma$, will increase the accuracy of the scheme. Several attempts have been made in order to lower the applied value of $\gamma$ and consequently decrease the numerical dissipation of the flux calculation method for subsonic flows such as channel flow simulation (Bui [5] and Ciardi *et al.* [6]), isotropic decaying turbulence (Ciardi *et al.* [6]), Bluff-body flows (Camarri *et al.* [7]), and also flow separation over an airfoil (Dahlström and Davidson [8], Tajallipour *et al.* [9]).

The self-adaptive upwinding technique considered in the present work is similar to the Monotonically Integrated LES (MILES) where both try to control the artificial dissipation but the latter decreases artificial dissipation by controlling the flux calculation. In MILES schemes the energy transfer from the resolved scales to the sub-grid scales is driven by the artificial dissipation of the discretisation scheme. Nevertheless, Garnier et al. [10] have presented poor results on decaying isotropic turbulence, showing how the accuracy of the MILES approach is strongly dependant on the specific discretisation scheme used. Further in MILES the artificial dissipation of the convective flux calculation scheme is not changed during the calculations while in the present self-adaptive upwinding scheme the artificial dissipation is decreased during the calculation by multiplying it with a factor which gets updated locally at each time step. The details of the self-adaptive upwinding scheme are given in the Numerical Method section.

In the present work the hydrodynamics characteristics of jets in cross-flow have been predicted and analyzed at the entrance and in the far fields of the jet using self-adaptive upwinding scheme with large eddy simulation based numerical scheme. First the stability of the solution has been checked to get the accurate predictions. The code is validated and calibrated with the experimental results of Andreopoulos and Rodi [1] in terms of hydrodynamics in cross-flow jets. After the code validations, the vertical structures generated at the near and far fields of the jet are analyzed and discussed.

## NOMENCLATURE

| | | |
|---|---|---|
| $\hat{A}$ | = | Jacobian matrix and |
| $C_S$ | = | Smagorinsky subgrid model's coefficient |
| $\vec{F}^{conv}$ | = | convective flux vector |
| $\rho$ | = | density |
| $u,v,w$ | = | Cartesian components of the velocity vector x,y,z directions |
| $T$ | = | temperature |
| $p$ | = | pressure |
| $\vec{n}_{ij}$ | = | the unit vector along the edge connecting nodes $i$ and $j$ |
| $\vec{X}_i$ | = | position vector of nodes i |
| $\beta$ | = | parameter used to calculate the inter nodal values in MUSCL scheme |
| $\gamma$ | = | parameter used to adjust the upwinding contribution in MUSCL scheme |
| $\theta$ | = | preset limit for the intensity of wiggles |
| $q$ | = | vector of conservative variables |
| $q_-, q_+$ | = | inter nodal values of the conservative variable vector for an edge |
| $\hat{q}$ | = | Roe average value of $q_-$ and $q_+$ evaluated at the boundary of a cell |
| $\varphi$ | = | vector of primitive variables |
| $\varphi_-, \varphi_+$ | = | inter nodal values of the primitive variable vector for an edge |

## NUMERICAL METHOD

The numerical method is a mixed finite volume-finite element method [11, 12] which has been developed to solve the unsteady Navier-Stokes equations. It operates on unstructured grids, using 2$^{nd}$ order MUSCL upwind formulation (βγ scheme) for the convective fluxes and a 2$^{nd}$ order finite element method for the diffusive fluxes. The subgrid scale terms are modeled by the Smagorinsky model. The value of Smagorinsky constant is used as $C_S$ = 0.01. For time discretization a second order implicit scheme is used. Ideal gas law for air is used to close the system of equations and the molecular viscosity is calculated using the Sutherland equation for air. The system of equations is solved using an iterative GMRES solver and using MPI parallel programming method [13]. The boundary values between the processes are exchanged with MPI.

### A. Self-Adaptive Upwinding Scheme

The self-adaptive scheme developed in [9] is reviewed herein. The Roe-MUSCL method for the convective flux calculations is first described. The normal component of the inviscid flux at the boundaries of neighboring cells is defined as a sum of an average term calculated by fluxes of two nodes belonging to the edge which the flux is calculated along it and an upwinding term

$$\vec{F}^{conv} \bullet \vec{n}_{ij} = \frac{1}{2}(\vec{F}^{conv}(q_+) + \vec{F}^{conv}(q_-)) \bullet \vec{n}_{ij} - \frac{1}{2}\left|\hat{A}(\hat{q},\vec{n}_{ij})\right|(q_+ - q_-) \tag{1}$$

where $\hat{q}$ is the average value of $q$ evaluated at the boundary of a cell or control volume using Roe method. $q_-$ and $q_+$ are calculated by interpolating the numerical flux of those two nodes to the boundaries of the cell $\partial C_i$ (inter nodal values between nodes i and j):

$$q_- = q_i + \frac{1}{2}[(1-\beta)(q_j - q_i) + \beta(\vec{\nabla} q)^L_{ij} \bullet \vec{n}_{ij}] \tag{2}$$

$$q_+ = q_j - \frac{1}{2}[(1-\beta)(q_j - q_i) + \beta(\vec{\nabla} q)^R_{ji} \bullet \vec{n}_{ij}] \tag{3}$$

This approach is used in order to improve the precision of the method without changing the approximation space [11, 12]. The parameter β determines to what extent central interpolation is used in order to calculate $q_+$ and $q_-$. As mentioned in Ref. 4, the value of β has been set as 1/3 in order to minimize the dissipative and dispersive errors. $(\vec{\nabla} q)^L_{ij}$ and $(\vec{\nabla} q)^R_{ji}$ are defined as left hand and right hand gradients (Figs. 1a, b). These gradients are computed respectively on the upstream ($L$) and downstream ($R$) tetrahedrons associated with edge ij (Fig. 1a). Local average gradients also can be used in Eqs. (2, 3) as an approximation. This is an extension of the MUSCL method to the finite element, because the gradients of the variable vector ($q$) are computed using the finite element technique.

Though Roe-MUSCL has predicted fairly accurate results for Euler or laminar simulations but it has been found too dissipative for LES [5, 7]. In order to control the amount of Roe upwinding dissipation a coefficient ($\gamma$) is introduced in equ. (1):

$$\vec{F}^{conv} \bullet \vec{n}_{ij}. = \frac{1}{2}(\vec{F}^{conv}(q_+) + \vec{F}^{conv}(q_-)) \bullet \vec{n}_{ij} - \gamma\left\{\frac{1}{2}\left|\hat{A}(\hat{q},\vec{n}_{ij})\right|(q_+ - q_-)\right\} \quad (4)$$

where $\gamma$ can vary between 0 and 1 ($\gamma$ = 0 corresponds to central differencing, and $\gamma$ = 1 corresponds to the full MUSCL-Roe method). Omitting the Roe upwinding term altogether ($\gamma$ = 0) causes all calculations to be unstable therefore for a given grid size, a minimum amount of upwinding dissipation is always required in order to provide stability. Therefore, a finer grid would require for a smaller value of $\gamma$.

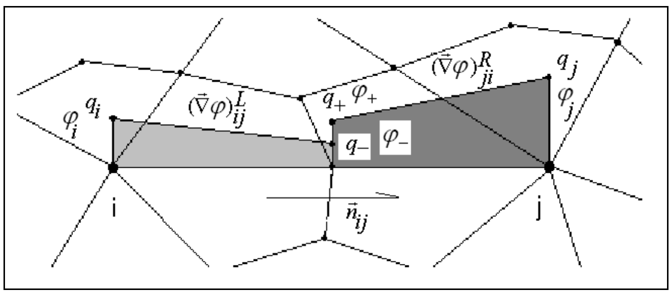


Fig. 1a Control volumes and convective flux calculation (Tajallipur et al., [9]).

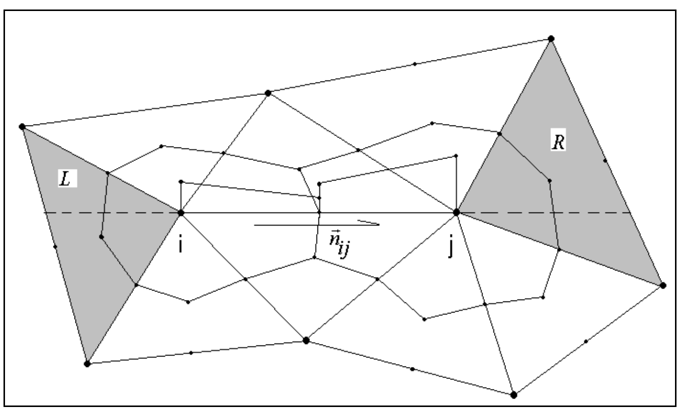


Fig. 1b Convective flux calculation (Tajallipur et al., [9]).

In order to determine and adjust upwinding parameter ($\gamma$) dynamically, a wiggle detector has been implemented. It checks to see if the intensity of the local wiggle is higher than a preset value. If this is the case then the scheme increases $\gamma$ linearly towards the full MUSCL-Roe scheme. Otherwise the scheme is more centered and $\gamma$ is decreased.

The wiggle definition of Ref. 8 has been extended in [9] to our numerical method as follows. A wiggle is assumed to be present along an arbitrary edge, if the coefficient of direction changes twice along the edge in that direction. That is, if for any flow variable $\Phi\ (\Phi \in [\rho,u,v,w,p])$

$$(\Phi_i - \Phi_{i-1})(\Phi_{i+1} - \Phi_i) < 0 \quad (5)$$

$$(\Phi_{i+2} - \Phi_{i+1})(\Phi_{i+1} - \Phi_i) < 0 \quad (6)$$

are true, then a wiggle is present. It can be describe from Fig. 1b, here a wiggle can be seen along the edge connecting nodes i and i+1, while there is no wiggle along the edge connecting nodes i-1 and i.

A new method developed by Tajallipour et al. [9] has been implemented for a more general and appropriate approach for the purpose of LES. The inequalities in Eqs. (5, 6) has been replaced by the followings:

$$[(\vec{\nabla}\Phi)^{L}_{ij} \bullet \vec{\boldsymbol{n}}_{ij}][(\vec{\nabla}\Phi)^{C} \bullet \vec{\boldsymbol{n}}_{ij}] = [(\vec{\nabla}\Phi)^{L}_{ij} \bullet \vec{\boldsymbol{n}}_{ij}][(\Phi_j - \Phi_i)/|\vec{\boldsymbol{X}}_j - \vec{\boldsymbol{X}}_i|] < \boldsymbol{\theta} \le 0 \quad (7)$$

$$[(\vec{\nabla}\Phi)^{R}_{ji} \bullet \vec{\boldsymbol{n}}_{ij}][(\vec{\nabla}\Phi)^{C} \bullet \vec{\boldsymbol{n}}_{ij}] = [(\vec{\nabla}\Phi)^{R}_{ji} \bullet \vec{\boldsymbol{n}}_{ij}][(\Phi_j - \Phi_i)/|\vec{\boldsymbol{X}}_j - \vec{\boldsymbol{X}}_i|] < \boldsymbol{\theta} \le 0 \quad (8)$$

If inequalities in Eqs. (7, 8) are satisfied then the intensity of the wiggle is more than the preset value ($\theta$) and $\gamma$ should be increased. This increment is a linear function of $\theta - Min\{[(\vec{\nabla}\Phi) \bullet \vec{n}_{ij}][(\vec{\nabla}\Phi)^{C} \bullet \vec{n}_{ij}]\}$. While, when inequalities (7,8) are not satisfied, the intensity of the wiggle is less than the preset value ($\theta$) and $\gamma$ can be decreased. This time, the decrement would be a linear function of $Max\{[(\vec{\nabla}\Phi) \bullet \vec{n}_{ij}][(\vec{\nabla}\Phi)^{C} \bullet \vec{n}_{ij}]\} - \theta$. In both linear functions, $(\vec{\nabla}\Phi) \in [(\vec{\nabla}\Phi)^{L}_{ij}, (\vec{\nabla}\Phi)^{R}_{ji}]$, $\Phi \in [\rho, u, v, w, p]$ the value of ($\gamma$) is chosen between 0 and 1. The value of $\theta$ is either negative or zero and usually has a small absolute value (≈ –0.00001 to –0.0001). The idea is to use the products of the gradients as a way to measure the intensity of a local wiggle. In case of LES, the situation is different then the DNS (where the grid is fine enough to capture the smallest scales of eddies present in the flow field) because even in the best cases, the cutoff mode is expected to fall within inertial sub-range and therefore there will be some energy in the highest scales which are expected to be captured by the simulation. Therefore, $\theta$ is replaced by a negative and relatively small value which will represent the existence of energy in the smallest scales and by changing the value of $\theta$, the amount of that energy is adjusted.

## PROBLEM DESCRIPTION

The most important parameter besides Reynolds number characterizing mixing in the configurations under investigation is the velocity ratio computed from the bulk velocities of the two fluid streams. This ratio determines the level of shear between the two streams and is defined as R = $u_j/u_{cf}$ (assuming density is constant). The base configuration investigated in this work was chosen to resemble the setup of Andreopoulos and Rodi [1] with R = 0.5. The jet issues perpendicular from a D = 50 mm pipe with $u_j$ = 6.95 m/s into a cross-stream approaching along a flat plate with $u_{cf}$ = 13.9 m/s (Fig. 2). The corresponding Reynolds number based on the jet velocity and pipe diameter is 20,500.

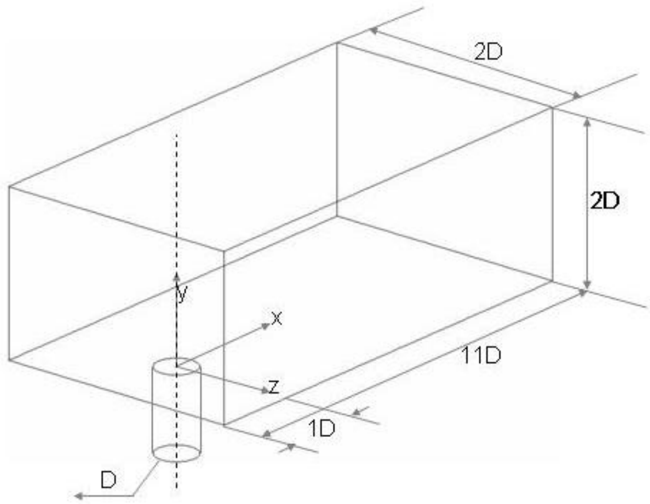


Fig. 2 Schematic of the problem.

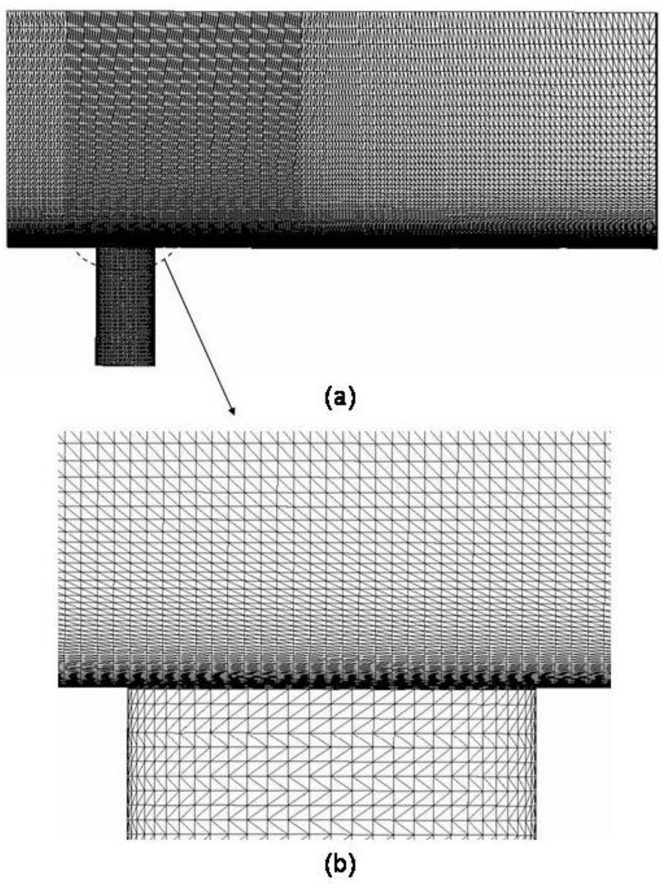


Fig. 3 (a) Unstructured grid for the geometry considered, and (b) magnified mesh topology near the jet and cross-flow interaction.

The actual wind tunnel can not be simulated using LES therefore the computational domain has been reduced from that of the wind tunnel used by Andreopoulos and Rodi [1]. A flow domain of 13D x 6D x 4D (stream-wise, wall-normal and span-wise) has been considered as the jet velocity considered is very small and it does not penetrate and spread far into the crossflow stream (Fig. 2). An unstructured tet/hybrid grid is used to model the pipe. The extensions of the computational domain along with the grid resolution are listed in Fig. 3. The total domain considered is represented with 6,610,000 elements and 1,140,000 nodes. The grid was clustered around the jet exit.

The inflow boundaries were treated as follows. At the jet pipe and the cross-flow boundaries velocity inlets the uniform velocity profiles have been considered. At the lateral boundaries a pressure far-field condition is applied and a Neumann condition is used for the outlet. On the solid walls a no-slip condition is applied with no special wall treatment for the SGS model. The boundary layer is resolved on the computational mesh which we have achieved by putting one grid point in the viscous sub-layer. The $y^+$ value evaluated for wall shear stress during the simulation showed that the distance of the wall next point is $\approx$ 2.

A time step size has been chosen to get CFL $\approx$ 1. The computations have been carried out till the turbulent flow fields are fully developed. The simulations are run for further flow through times (based on the cross-flow velocity) and statistics were sampled during this time.

## RESULTS AND DISCUSSION

The results of the self-adaptive upwinding large eddy simulations are compared to the experimental data of Andreopoulos and Rodi [1] and numerical predictions (FLUENT predictions) of Wegner et al. [2] to understand the ability of the LES computations to precisely capture the fluid hydrodynamics in the investigated configuration.

First a qualitative overview on the flow field is given in Figs. 4 and 5. The mean flow streamlines in the jet exit region are shown in Fig. 4. From Fig. 4 it can be seen that there is a vortices inside the jet pipe, whose center is located $\approx$ 0.1D in the jet pipe. The vortex originated from the collision of the jet and the cross-flow shear layers. A strong interaction of jet and cross-flow in the jet exit region can be seen. A similar phenomenon is also reported by Andreopoulos and Rodi [1] for R = 0.5 at z/D = 0. A similar observation is also reported by the Kelso et al. [14] for low Reynolds number. The bending of the jet is started in the jet pipe and nearly completed at x/D = 1.0), which results into the lifting of the cross-flow over the jet. Further the separation of cross-flow boundary layer can be seen by the way of vortex just upstream of the jet exit. Some jet pipe fluid is being entertained in this vortex.

Fig. 5 shows an evolution of a counter-rotating vortex pair (CVP) at various distances from the jet exit A small CVP can be seen at the jet exit (x/D = 0.0), which also support the idea that it is initiated by the pipe vorticity. At x/D = 0.5 and 1.0 the upward and outward deflection of cross-flow by the bent-over jet can be seen clearly. Further downstream the CVP grows and it spreads in the flow domain.

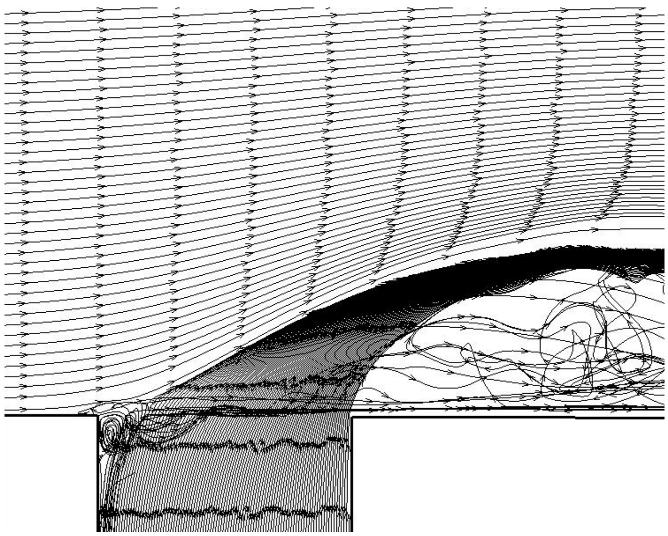

Fig. 4. The streamlines of the mean velocities in the symmetry plane.

The mean axial and wall-normal velocity profiles in the jet symmetry plane (z/D = 0) are provided in Figs. 6–7. To have a better understanding and comparison of the velocity profiles in axial and wall–normal direction have been scaled. The mean axial and wall-normal velocity profiles computed in the present work are qualitatively in good agreement with the experimental data [1] and numerical predictions of Wegner et al. [2]. From Fig. 6a it can be seen that the LES shows a negative axial velocity at x/D = –0.5 which is due to the existence of a recirculation bubble upstream of the jet orifice, which is also reported by Wegner et al. [2]. A similar observation of recirculation from LES can be made at x/D = 1 (Fig. 6f), which is not reported by Andreopoulos and Rodi [1] in their experimental measurements. However, Andreopoulos and Rodi [1] reported that in the lee of the jet with similar parameters a reveres flow region forms very close to the wall in which measurement is not possible. The presence of recirculation zone is also supported by the observations of Foss [15] which clearly shows a recirculation. In LES there is no backflow downstream of x/D = 2.0 and the flow profiles are in good agreement with the experimental measurements of Andreopoulos and Rodi [1]. Similarly, the flow profiles in the wall-normal direction (Fig. 7) are in good agreement in the jet exit region. In the region downstream of the jet exit, influenced by large-scale structures, the wall-normal velocity values are over-predicted while as we go further downstream the wall-normal velocity values are in good agreement.

The velocity profiles obtained from the LES simulations from the present work are also compared with the work of Wegner et al. [2], who has carried out LES simulation of jet in cross-flows using FLUENT (CFD software). From the Figs. 6–7 it can be seen that the results are qualitatively in agreement with the Wenger et al's predictions. However quantitatively present LES predictions using self-adaptive upwinding are in good agreement with the experimental measurements as compared to the LES predictions of Wegner et al. [2]. The self-adaptive Upwinding scheme used in the present work is the average upwinding coefficient decreases from 1.0 to about 0.06 which is resulting in a significant decrease in the introduced numerical dissipation there exist more eddies in the simulated flow. Since eddies are not diffused when the self-adaptive upwinding method is applied and therefore fluctuations are more preserved by the numerical scheme. The increase in diffusion due to numerical scheme is removed by decreasing the upwinding's coefficient and therefore the overall amount of numerical dissipation decreases. Therefore the numerical scheme is less dissipative and large scale eddies are better captured which results into more accurate predictions.

The span-wise velocity profiles are plotted in Fig. 8 at z/D = -0.5. At the symmetry plane the W-values are very small which is also reported by the Andreopoulos and Rodi [1] in their experimental measurements. From Fig. 8 it can be seen that the span-wise velocity values are negative near the exit, due to the deflection of cross-stream around the jet near the wall. At x/D = 0.5 the induced outward motion is fairly strong as the lateral velocity reaches a maximum value of $0.385U_{inf}$. At the downstream of the jet exit, the low pressure in the wake region induces the inward flow which in results changes the sign of span-wise velocity values near the wall. The outward flow in the wall-normal direction and the inward flow near the wall are part of the vortex motion.

A qualitative and quantitative comparison of turbulent kinetic energy "*k*" with experimental data of Andreopoulos and Rodi [1] and numerically predicted data of Wegner et al. [2] are shown in Fig. 9. It can bee seen that the present LES predictions are in good agreement in the jet exit region, while in the region downstream of the jet exit the present numerically predicted values are higher than the experimental data[1], while the qualitative agreement is fairly good.. As mentioned by Wegner et al. [2], the turbulent fluctuations are over-predicted due to the influence of large-scale structures which is also applicable to the present predictions. In their work, Andreopoulos and Rodi [1] have mentioned that (i) the hotwire anemometry employed for their measurements in general tends to underestimate turbulence quantities, (ii) the error in experimental measurements for the velocity fluctuations as high as 10%, and (iii) the experimental boundary conditions are not mentioned very well. These arguments are also applies for the deviation in velocity profiles reported in the present work.

However, the predictions of turbulent quantities in the present work are closer to the experimental data as compared to the numerical data of Wegner et al. [2]. This is because the self-adaptive upwinding scheme applied in the present work, which significantly decreases the upwinding coefficient at the far fields from the jet's inlet.

## CONCLUSIONS

The jet in cross-flow is studied using large eddy simulation on an unstructured mesh using self-adaptive upwinding scheme. An unstructured finite-volume/finite-element flow solver which uses the Roe-MUSCL flux calculation scheme, the Van Leer-Val Albada limiter function and the self-adaptive upwinding method was used in the simulations. The applied self-adaptive scheme regulates the numerical dissipation by adjusting the upwinding term through a sensor that locally estimates the intensity of wiggles in the flow variables. It was shown that the self-adaptive scheme was more successful than the full upwinding method in predicting fluid hydrodynamics in near and far fields of the jets. The LES also reproduced many phenomena present in such a flow, like the shear layer ring vortices and the counter-rotating vortex pair. It was observed that lowering the amount of upwinding preserves the unsteady large eddy scales in the flow field. A comparison has been made with the experimental data reported in the literature and a reasonable agreement with the measurements was obtained. In the present work an intense back-flow near the flat wall is observed, which has not been reported experimentally. The presence of recirculation is in agreement with the work of Wegner et al. [2], but in both cases it is predicted too high above the wall and probably too intense.

As a next step we are in the process of implementing the turbulent inflow conditions at the inlet boundaries to further understand the flow hydrodynamics in the near and far fields of the jets. Also the comparison of predictions for shear stress, stability parameters, structural parameters and turbulent kinetic energy production and advection using self-adaptive upwinding scheme with existing fully upwinding scheme is under progress.

## ACKNOWLEDGMENTS

This work was supported in part by the Natural Sciences and Engineering Research Council of Canada (NSERC).

## REFERENCES

[1] Andreopoulos, J., Rodi, W., “Experimental investigation of jets in a cross-flow”, *J. Fluid Mechanics*, Vol. 138, 1984, pp. 93–127.

[2] Wegner, B., Huai, Y., Sadiki, A., “Comparative study of turbulent mixing in jet in cross-flow configurations using LES”, *Int. J. Heat Mass Transfer*, Vol. 25, 2004, pp. 767–775.

[3] Majander, P., Siikonen, T., “Large-eddy simulations of a round jet in a cross-flow”, *Int. J. Fluid Flow*, Vol. 27, 2006, pp. 402–415.

[4] Carpentier, R., “Comparaison Entre des Schémas 2D de Type Roe Sur Maillages Régulier Triangule ou Quadrangle, II: Calcul au Sommet-le βγ Schéma,” Institut National de Recherche en Informatique et en Automatique (INRIA), Rept. 3360, France, Feb. 1980.

[5] Bui, T. T., “A Parallel, Finite-Volume Algorithm for Large Eddy Simulation of Turbulent Flows,” Dryden Flight Research Center, California, NASA TM-206570, Jan. 1999.

[6] Ciardi, M., Saugaut, P., Klein, M., Dawes, W.N., “A Dynamic Finite Volume Scheme for Large-Eddy Simulation on Unstructured Grids,” *J. of Comp. Physics*, Vol. 210, 2005, pp. 632-655.

[7] Camarri, S., Salvetti, M.V., “Large-Eddy Simulation of a Bluff-Body Flow on Unstructured Grids,” *International Journal for Numerical Methods in Fluids*, Vol. 40, 2002, pp. 1431-1460.

[8] Dahlström , S., Davidson, L., “Large Eddy Simulation Applied to a High Reynolds flow Around an Airfoil Close to Stall,” *41st AIAA Aerospace Sciences Meeting and Exhibit*, Chalmers University of Technology, Sweden, 2003.

[9] Tajallipour, N., Owlam, B.B., Paraschvoiu, M., “Self-Adaptive Upwinding for Large Eddy Simulation of Turbulent Flows on Unstructured Elements,” *Journal of Aircraft*, Vol. 46, May – June 2009, pp. 915–926.

[10] Garnier, E., Mossi, M., Sagaut, P., Comte, P., Deville, M., “On the use of shock-capturing schemes for large-eddy simulation,” *Journal of Computational Physics*, Vol. 153, 1999, 273–311.

[11] Cadiou, A., “NadiaLES: Theoretical Manual,” Centre National De La Recherche Scientifique (CNRS), Rept. LMFA-UMR CNRS 5509, France, 2003.

[12] Hallo, L., Le, C., Buffet, Ribault and M., “An Implicit Mixed Finite-Element-Finite-Volume Method for Solving 3-D Turbulent Compressible Flows,” *International Journal for Numerical Method in Fluids*, Vol. 25, 1997, pp.1241-1261.

[13] Snir, M., Otto, S., Lederman, S. H., Walker, D., Dongarra, J., *MPI-The Complete Reference*, The MIT Press, Vol. 1, 2nd edition, Massachusetts Institute of Technology, Cambridge, London, England, 1998.

[14] Kelso, R., Lim, T., Perry, A., “An experimental study of round jets in cross-flow”. *J. Fluid Mechanics*, Vol. 306, 1996, pp. 111–144.

[15] Foss, J., “Interaction region phenomena for the jet in a cross-flow problem”, In: Report SFB 80/E/161, University of Karlsruhe.

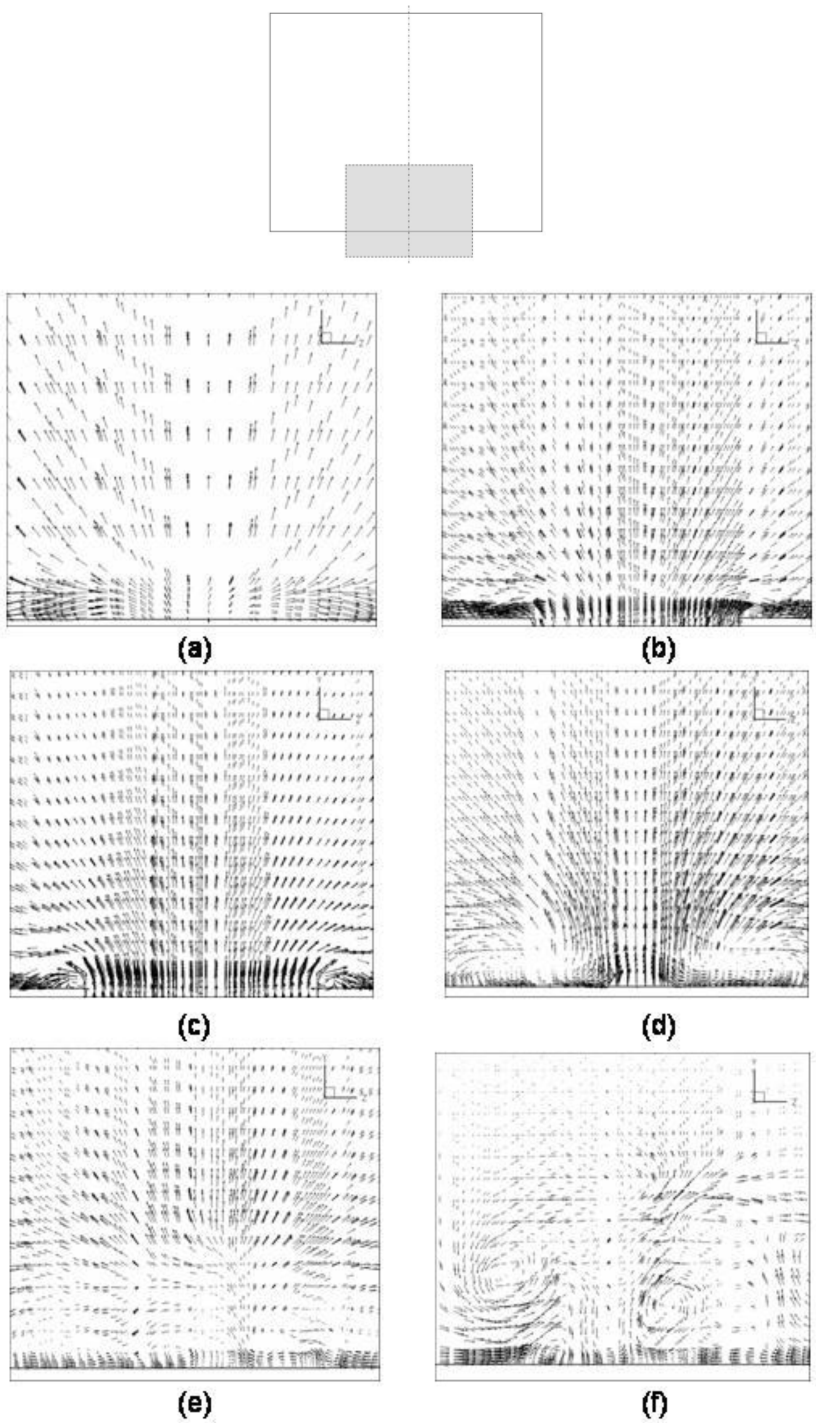

Fig. 5. Counter-rotating vortex at stream-wise planes at various distances from the jet exit (a) x/D = -0.5, (b) x/D = -0.25, (c) x/D = 0.0, (d) x/D = 0.5, (e) x/D = 1.0, and (f) x/D = 2.0.

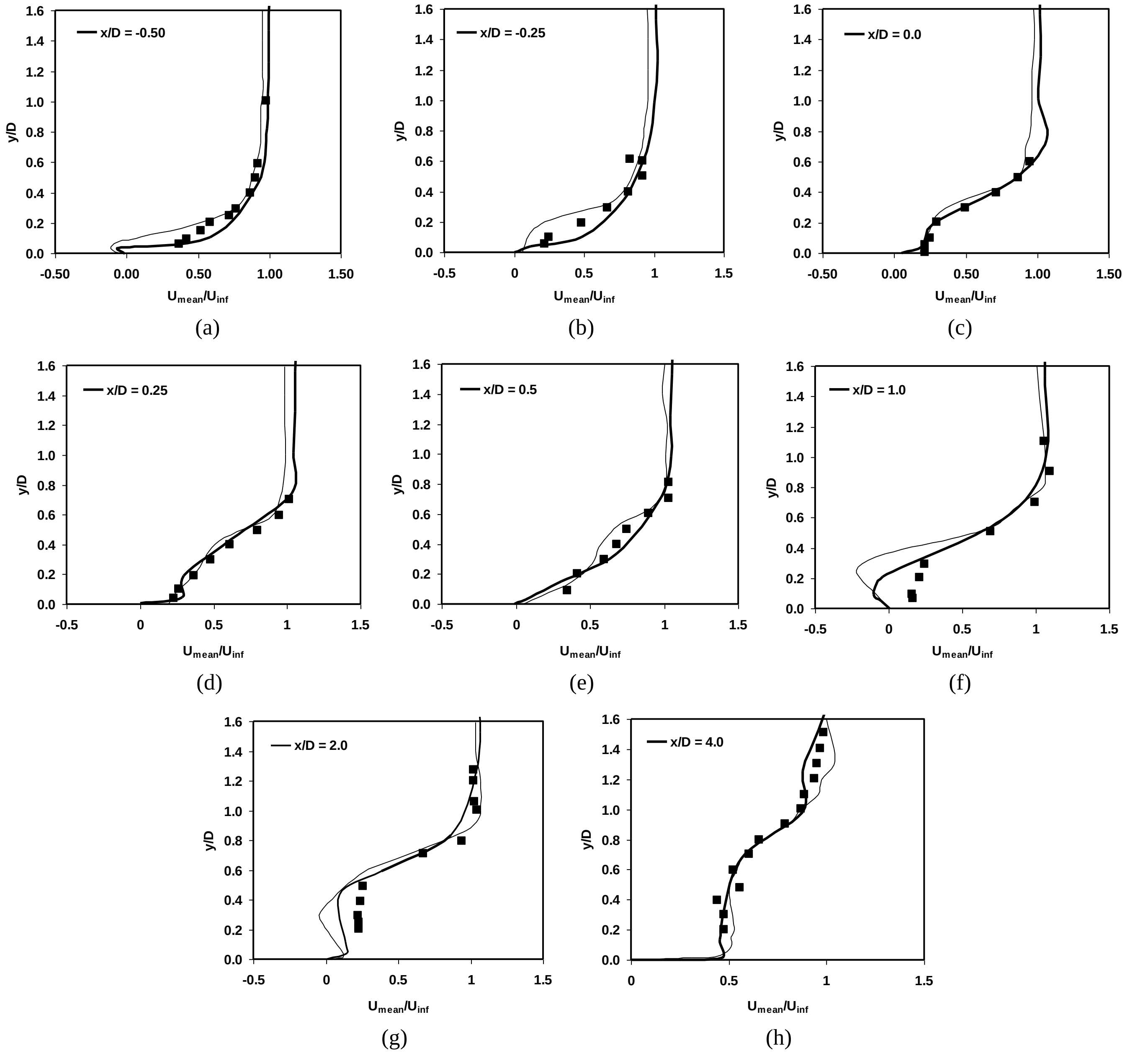


Fig. 6. Mean axial velocity: LES LES (solid line), Wegner et al. (2004) (dashed line), and experimental data from Andreopoulos and Rodi (1984) (■)

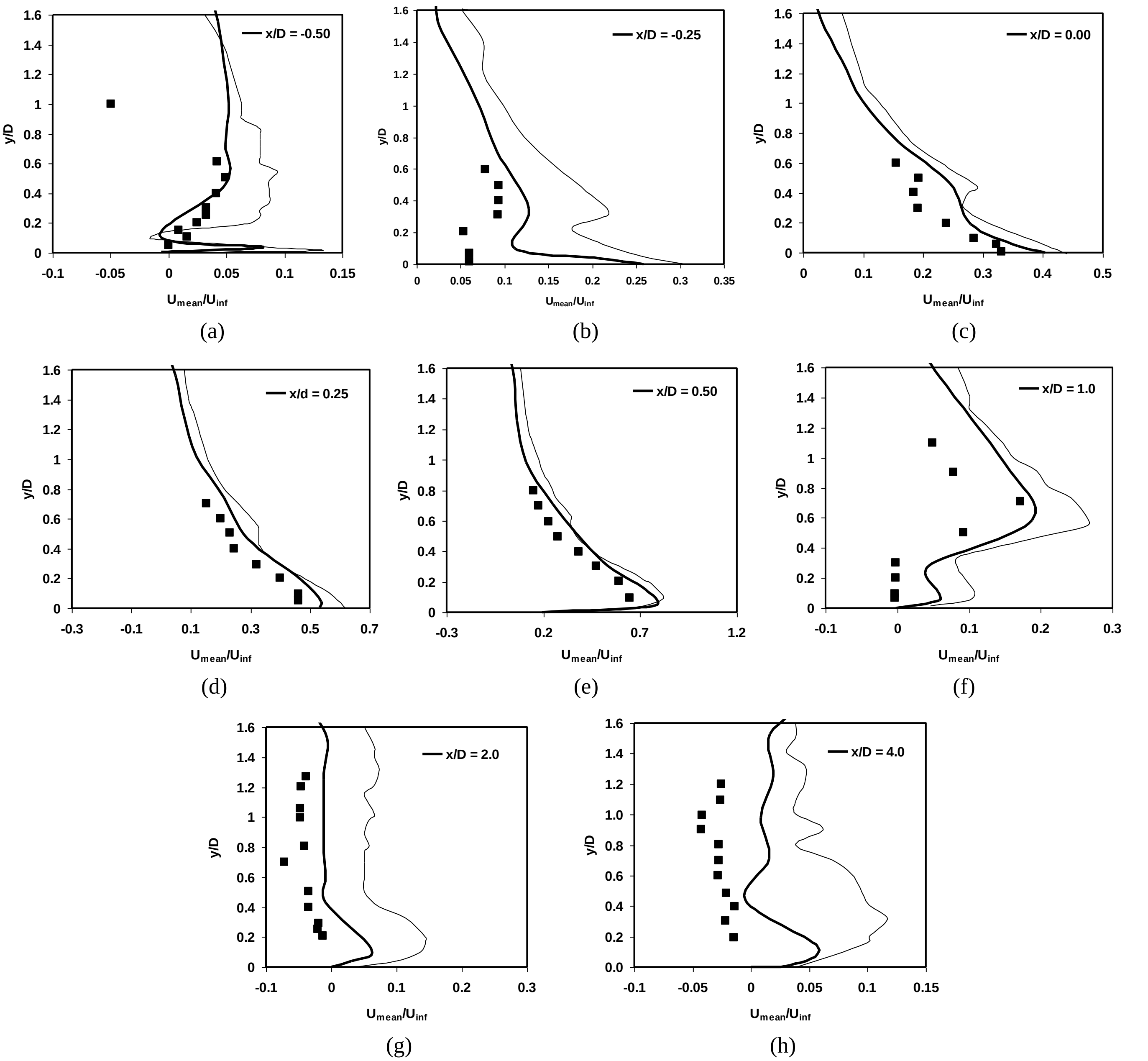


Fig. 7. Mean wall-normal velocity: LES (solid line), Wegner et al. (2004) (dashed line), and experimental data from Andreopoulos and Rodi (1984) (■)

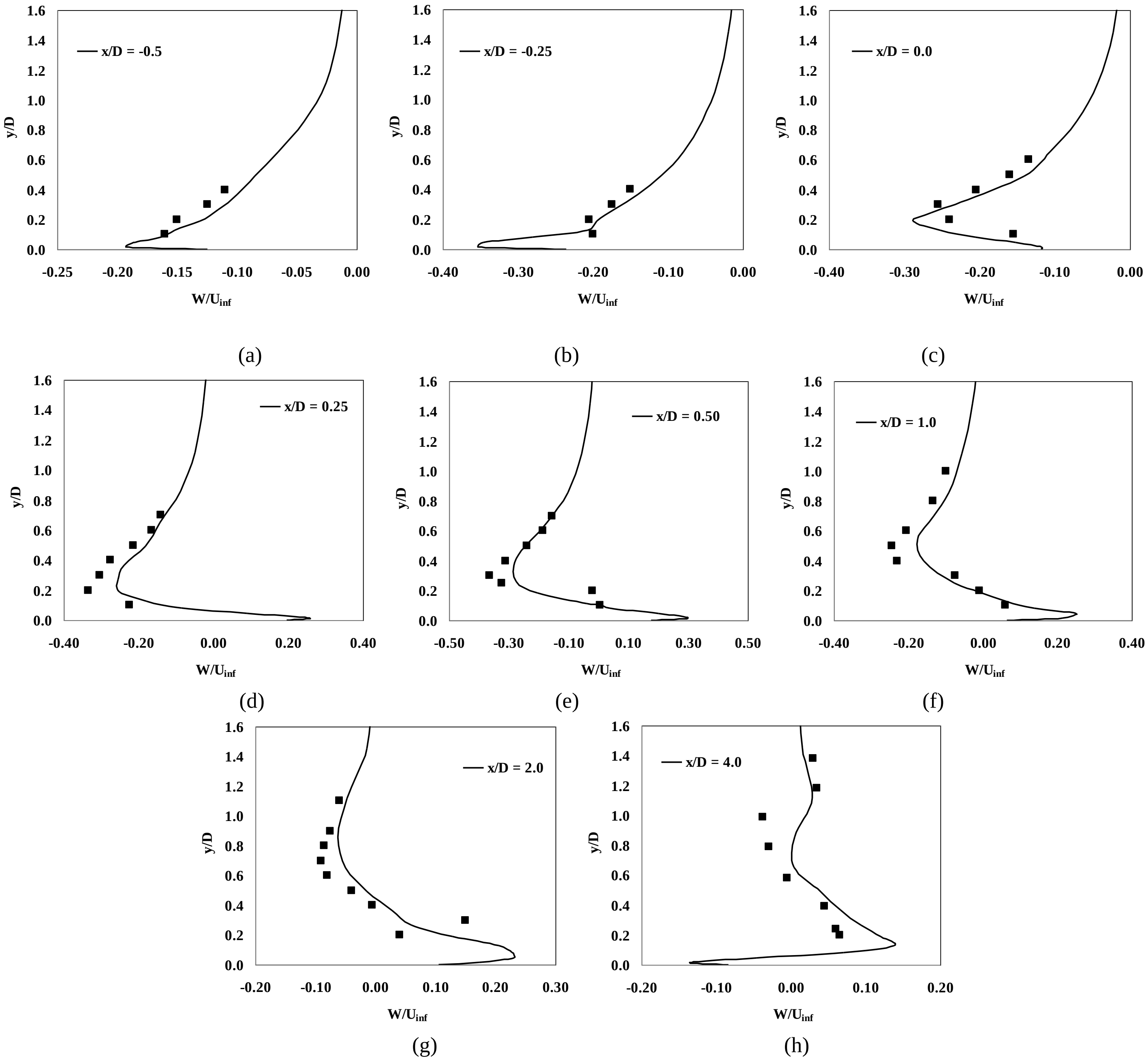


Fig. 8. Mean W velocity profiles: LES (solid line), and experimental data from Andreopoulos and Rodi (1984) (■)

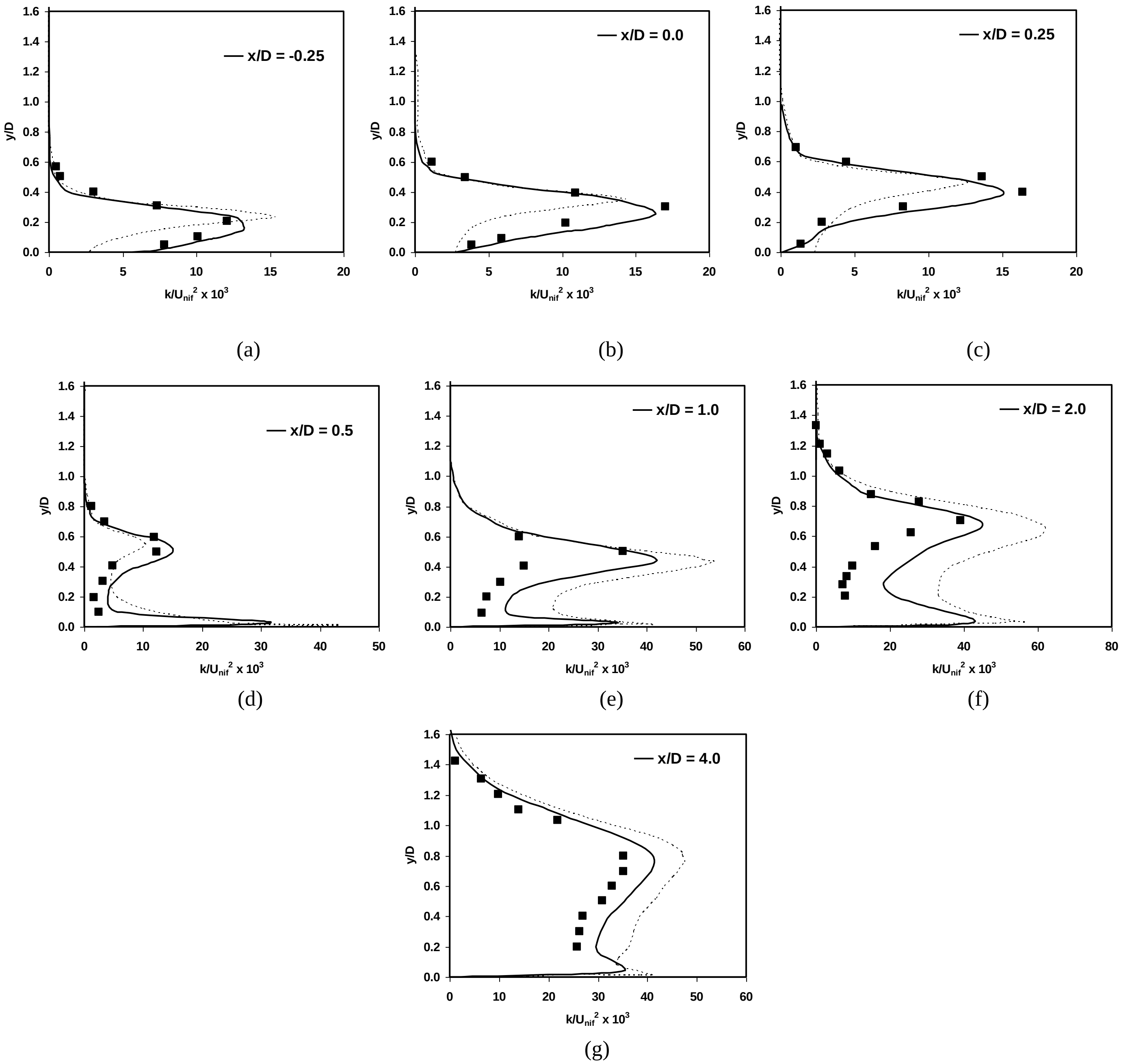


Fig. 9. Turbulent kinetic energy: LES (solid line), Wegner et al. (2004) (dashed line), and experimental data from Andreopoulos and Rodi (1984) (■).